AZD5438, a potent oral inhibitor of cyclin-dependent kinases 1, 2, and 9, leads to pharmacodynamic changes and potent antitumor effects in human tumor xenografts

Kate F. Byth,[2] Andrew Thomas,[1] Gareth Hughes,[1] Cheryl Forder,[1] Alexandra McGregor,[1] Catherine Geh,[1] Sandra Oakes,[1] Clive Green,[1] Mike Walker,[1] Nicholas Newcombe,[1] Stephen Green,[1] Jim Growcott,[1] Andy Barker,[1] and Robert W. Wilkinson[1]

[1]AstraZeneca Pharmaceuticals, Macclesfield, Cheshire, United Kingdom and [2]AstraZeneca R&D Boston, Waltham, Massachusetts

Abstract

Deregulation of the cell cycle has long been recognized as an essential driver of tumorigenesis, and agents that selectively target key cell cycle components continue to hold promise as potential therapeutics. We have developed AZD5438, a 4-(1-isopropyl-2-methylimidazol-5-yl)-2-(4-methylsulphonylanilino) pyrimidine, as a potent inhibitor of cyclin-dependent kinase (cdk) 1, 2, and 9 (IC_{50}, 16, 6, and 20 nmol/L, respectively). *In vitro*, AZD5438 showed significant antiproliferative activity in human tumor cell lines (IC_{50} range, 0.2–1.7 μmol/L), causing inhibition of the phosphorylation of cdk substrates pRb, nucleolin, protein phosphatase 1a, and RNA polymerase II COOH-terminal domain and blocking cell cycling at G_2-M, S, and G_1 phases. *In vivo*, when orally administered at either 50 mg/kg twice daily or 75 mg/kg once daily, AZD5438 inhibited human tumor xenograft growth (maximum percentage tumor growth inhibition, range, 38–153; $P < 0.05$). *In vivo*, AZD5438 reduced the proportion of actively cycling cells. Further pharmacodynamic analysis of AZD5438-treated SW620 xenografts showed that efficacious doses of AZD5438 (>40% tumor growth inhibition) maintained suppression of biomarkers, such as phospho-pRbSer^{249}/Thr^{252}, for up to 16 hours following a single oral dose. A comparison of different schedules indicated that chronic daily oral dosing provided optimal cover to ensure antitumor efficacy. These data indicate that broad cdk inhibition may provide an effective method to impair the dysregulated cell cycle that drives tumorigenesis and AZD5438 has the pharmacologic profile that provides an ideal probe to test this premise. [Mol Cancer Ther 2009;8(7):1856–66]

Introduction

In virtually all tumors, gene amplifications and/or deletions or functional alterations of key regulators contrive to deregulate the cyclin D1-cyclin-dependent kinase (cdk) 4/p16/pRb/E2F signaling axis (1) and, in the case of p27 and cyclin E, have prognostic value (2, 3). These observations have placed cdks among the most highly attractive targets for therapeutic intervention in cancer (4).

The conventional view of cdk signaling (reviewed in refs. 5, 6) has evolved to incorporate novel activities of cyclin-cdk complexes that have been observed in response to certain conditions, particularly when specific cdks are depleted (reviewed in ref. 7). It seems that functional redundancy among cdks and cyclin binding partners is a frequent event bringing clear implications for the clinical utility of selective cdk inhibition. Promiscuity among cdk-cyclin binding partners has been observed both *in vivo* and *in vitro* and could drive resistance in the clinic (8, 9), with a growing number of studies indicating that highly selective cdk inhibition may not be therapeutically effective.

Hence, agents that simultaneously target a range of cdks are more likely to be successful clinically than selective cdk inhibitors, providing that an acceptable therapeutic margin can be achieved (4). Which combination of cdk targets would likely have greatest therapeutic benefit? Selective cdk4 inhibitors are cytostatic *in vitro*, a phenotype more likely to produce stable disease than clinical responses. However, cdk4 inhibition *in vivo* results in tumor regression (10). Targeting cdk2 has the potential to trigger apoptosis, particularly where E2F-1 activity is already high (11). Despite the lack of selective cdk1 inhibitors being described, dual cdk1-cdk2 inhibitors have been reported (12–14) and combined depletion of cdk1 and cdk2 is more proapoptotic than depletion of either cdk alone (9). cdk1 also has the attraction that it can regulate the activity of survivin (BIRC5), which has been implicated in regulation of the spindle checkpoint and inhibition of apoptosis and is selectively expressed in the majority of human tumor types (15). Inhibition of cdk1 rapidly down-regulates survivin expression-inducing MYC-dependent apoptosis, leading to the suggestion that cdk1 inhibition might be a useful therapy for tumors that overexpress MYC, for example, in Burkitt's lymphoma (16). cdk7 and cdk9 play roles in transcriptional regulation through

Received 8/29/08; revised 3/30/09; accepted 4/5/09; published OnlineFirst 6/9/09.

The costs of publication of this article were defrayed in part by the payment of page charges. This article must therefore be hereby marked *advertisement* in accordance with 18 U.S.C. Section 1734 solely to indicate this fact.

Note: This article is dedicated to our late colleague F. Thomas Boyle.

Requests for reprints: Kate F. Byth, AstraZeneca R&D Boston, 35 Gatehouse Drive, Waltham, MA 02451. Phone: 781-839-4144; Fax: 781-839-4200. E-mail: Kate.Byth@AstraZeneca.com

doi:10.1158/1535-7163.MCT-08-0836

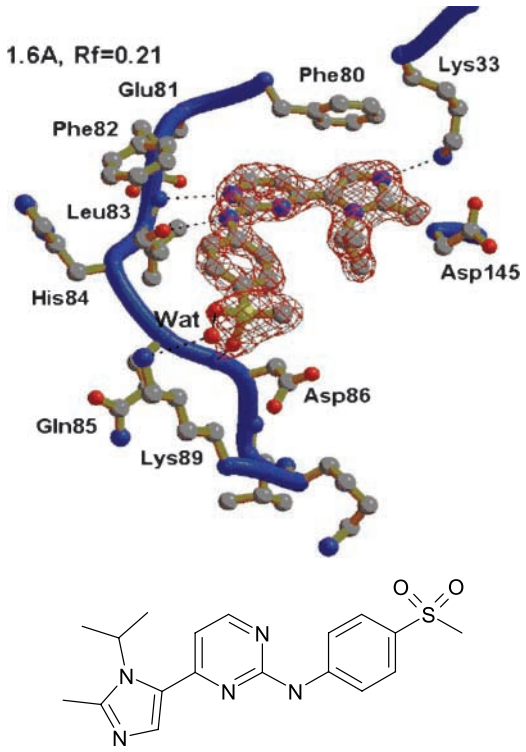

Figure 1. Crystal structure of AZD5438 bound to cdk2 complex. Binding mode is derived from X-ray structure determination of AZD5438 bound to the cdk2 complex at 1.6 Å resolution. This binding mode is typical of compounds from this imidazole series with hydrogen-bonding interactions with the hinge region of the protein being made between the pyrimidine N1 and Leu83 backbone NH and between the amino NH and Leu83 backbone carbonyl O; a third interaction between the imidazole N1 and the Lys33 amino group picks up the sugar pocket, whereas the sulfone tail points toward solvent and picks up an interaction with a water molecule.

phosphorylation of serines within the COOH-terminal domain (CTD) of RNA polymerase II. Cdk7-mediated phosphorylation of RNA polymerase II leads to promoter clearance, initiation of transcription, and recruitment of RNA capping enzymes. Subsequent phosphorylation by cdk9 (pTEFb) regulates productive transcript elongation (17, 18). Cyclin H-cdk7 is also a component of the cdk activating kinase and hence contributes to both cell cycle and transcriptional regulation (19). Both cyclin E-cdk2 and cyclin B-cdk1 are capable of phosphorylating the CTD *in vitro* and combined depletion of cdk2 and cdk1 by inducible short hairpin RNA reduces RNA polymerase II expression and CTD phosphorylation (9, 20, 21). Flavopiridol is a potent inhibitor of cdk9, and inhibition of expression of antiapoptotic proteins through decreased transcription of labile mRNAs encoding proteins such as Mcl-1 and XIAP may partly account for the activity of flavopiridol in chronic lymphocytic leukemia (4, 22).

Agents that simultaneously target cdk4 and cdk1/2 may be less effective therapeutically because the G_1 block induced by cdk4 inhibition can be antagonistic to the induction of apoptosis in S-G_2 phase. Further, exploiting the value of cdk9 inhibition through lowering the threshold for apoptosis induction indicates that a rational approach both to overcome potential redundancy and to optimize cell killing would be to develop a combined cdk1/cdk2/cdk9 inhibitor. Here, we describe, for the first time, the preclinical development of AZD5438, a novel orally bioavailable, cdk1, cdk2, and cdk9 inhibitor. AZD5438 caused growth inhibition in a range of human tumor xenografts and showed pharmacodynamic effects on cdk substrates both preclinically and in human volunteers (23).

Materials and Methods

Reagents

AZD5438, a 4-(1-isopropyl-2-methylimidazol-5-yl)-2-(4-methylsulphonylanilino) pyrimidine, was synthesized by AstraZeneca Pharmaceuticals (24).

Cell Lines

Human cancer cell lines for both *in vitro* and *in vivo* work were obtained from the American Type Culture Collection[3] and the European Collection of Animal Cell Cultures. Cells were grown in culture conditions as previously described (14). All culture medium was obtained from Life Technologies Cell Culture Systems, heat-inactivated FCS was from Life Technologies, and glutamine was from Sigma.

Recombinant Kinase Assays

The ability of AZD5438 to inhibit cdk activity was examined as previously described using a scintillation proximity assay with recombinant cdk-cyclin complexes of cyclin E-cdk2, cdk2-cyclin A, cdk4-cyclin D, and recombinant retinoblastoma substrate (amino acids 792–928) or cdk1-cyclin B1 with a peptide substrate derived from the *in vitro* p34cdc2 phosphorylation site of histone H1 (biotin-X-Pro-Lys-Thr-Pro-Lys-Lys-Ala-Lys-Lys-Leu; ref. 14). The activity of AZD5438 against recombinant cdk5/p25 (at 2 μmol/L ATP) was determined in a scintillation proximity assay–based assay using peptide substrate (AKKPKTPKKAKKL-OH). Inhibition of glycogen synthase kinase 3β activity was determined with scintillation proximity assay based on the use of human purified glycogen synthase kinase 3β enzyme and eukaryotic initiation factor 2B substrate (at 1 μmol/L ATP). AZD5438 was screened against active recombinant human cdk6-cyclin D3, cdk7-cyclin H/MAT1 (cdk activating kinase complex), and cdk9-cyclin T using the kinase selectivity screening service (KinaseProfiler) from Upstate Biotechnology.

Western Blotting

SW620 cells were exposed to a range of concentrations of AZD5438 for 2 h before preparation of cell lysates for Western blotting. For the nucleolin and protein phosphatase 1a (PP1a) studies, cells were arrested in mitosis with nocodazole for 16 h before treatment. The following antibodies were used: phosphospecific pRb [Biosource, and as previously described (14)]; total and Ser[3] phosphorylated

[3] http://www.lgcpromochem.com/atcc/

RNA Pol II (Covance); TG3, an antibody that cross-reacts with nucleolin only when phosphorylated by cdk1-cyclin B (Molecular Geriatrics Corp.; ref. 25); and total and phosphorylated PP1a (Cell Signaling Technology). Phosphohistone H3 (phH3; Millipore) and cyclin E (Santa Cruz Biotechnology) antibodies were used for *ex vivo* evaluation of xenograft lysates.

Measurement of Cell Proliferation

AZD5438 was tested against solid tumor cell lines as previously described (14). Briefly, cells were incubated for 48 h with AZD5438 at a range of concentrations. At the end of incubation, the cells were pulsed with 5-bromo-2′-deoxyuridine (BrdUrd) and the amount of DNA synthesis was measured. The IC_{50} for inhibition of proliferation was specifically determined independently of cell death. Multiple myeloma cell lines were seeded into 96-well plates in RPMI 1640 supplemented with 10% FCS and glutamine and dosed with AZD5438 for 72 h. Cell growth was measured using AlamarBlue (Invitrogen) and GI_{50} values were calculated with reference to pretreatment control values.

Cell Cycle Analysis by Fluorescence-Activated Cell Sorting

To determine the effect of AZD5438 on cell cycle, synchronous MCF-7 breast cancer cells (arrested by serum starvation for 24 h and then released into medium plus serum) and asynchronous MCF-7 were incubated with various concentrations of AZD5438 or DMSO control for 24 h at 37°C. After incubation, cells were pulsed with BrdUrd and samples were prepared as previously described (14) for fluorescence-activated cell sorting analysis.

In vivo Studies

Swiss nude (*nu/nu* genotype; AstraZeneca) mice and nude (Nude:Hsd Han:RNU-rnu; AstraZeneca) rats were bred and housed in negative pressure isolators (PFI Systems Ltd.) at Alderley Park, United Kingdom. Experiments were conducted on 8- to 12-wk-old female mice in full accordance with the UK Home Office Animal (Scientific Procedures) Act 1986. All human tumor xenografts except HX147 were established by s.c. injecting 100 μL of tumor cells (between 1×10^6 and 1×10^7 cells mixed 1:1 with Matrigel; Becton Dickinson). HX147 tumors were derived from fragment implants (1 mm^3 pieces) from tumors taken from mice initially implanted s.c. with 1×10^7 cells. These tumor fragments were passaged in mice thrice before implant for antitumor work. Tumors were measured up to three times per week with calipers, tumor volumes were calculated, and the data were plotted as geometric mean for each group versus time, as previously described (26). Animals were randomized into treatment groups (typically $n = 10$) when tumors reached a mean size of approximately >0.2 cm^3 and >0.5 cm^3 for mice and rats, respectively. AZD5438 was prepared in hydroxy-propyl-methyl-cellulose. Animals were given either AZD5438 (37.5–75 mg/kg) or vehicle control once or twice daily by oral gavage for ~3 wk in each case. Tumor volume and percentage tumor growth inhibition (% TGI) were calculated as described previously (26). Statistical analysis of any change in tumor volume was carried out using a standard t test ($P < 0.05$ was considered to be statistically significant).

Ex vivo Analysis

To determine the pharmacodynamic effects of AZD5438 treatment, groups of mice (typically $n = 3$) were humanely culled at intervals during efficacy studies and biosamples (e.g., blood and tumors) were removed. For BrdUrd labeling, mice were injected i.p. with 0.3 mL (200 mg/kg) BrdUrd (Sigma) at various time points before culling. For flow cytometry, cell suspensions were prepared from the snap-frozen tumors using an automated tissue disaggregation system (Medimachine, BD Biosystems) and fixed in 80% ethanol for a minimum of 24 h. Once fixed, tumor cell suspensions were immunolabeled and analyzed for BrdUrd uptake as described above. Flow cytometric determination of phH3 suppression in tumor cell suspensions was carried out as described elsewhere (27). For histologic analyses, tumors were fixed in 10% neutral buffered formalin for 24 to 48 h and then processed into paraffin wax blocks. Immunohistochemical assessment of cleaved caspase-3 was carried out as previously described (27).

For immunoblotting studies, frozen tumor samples were homogenized in 10-fold (v/w) Cell Extraction Buffer (Invitrogen) using the Spex 6850 cryogenic freezer/mill (Spex CertiPrep). Protein content of all tumor lysates was evaluated using Bio-Rad detergent-compatible protein assay reagents before SDS-PAGE electrophoresis and immunoblotting studies as described above.

For pharmacokinetic studies, plasma and tumor samples were processed and AZD5438 concentrations were determined by high-performance liquid chromatography-tandem mass spectrometry, essentially as described previously (28). Pharmacokinetic analysis of plasma and tumor

Table 1. Average IC_{50} values in μmol/L for AZD5438 activity against a panel of cdks *in vitro*

	cdk2-cyclin E	cdk2-cyclin A	cdk1-cyclin B1	cdk4-cyclin D1	cdk5-p25	cdk6-cyclin D3	cdk7-cyclin H	cdk9-cyclin T
AZD5438 IC_{50} (μmol/L)	0.006	0.045	0.016	0.449	0.014	0.021	0.821	0.020
n	10	3	6	3	2	1	1	1
Flavopiridol IC_{50} (μmol/L)	0.282	0.405	0.027	0.132	ND	0.395	0.514	0.011
n	6	3	2	6	—	1	1	1
R-roscovitine IC_{50} (μmol/L)	0.249	2.122	0.669	≥10	0.331	≥30	0.513	0.572
n	3	3	4	3	4	1	1	1

Abbreviations: n, number of repeats; ND, not done.

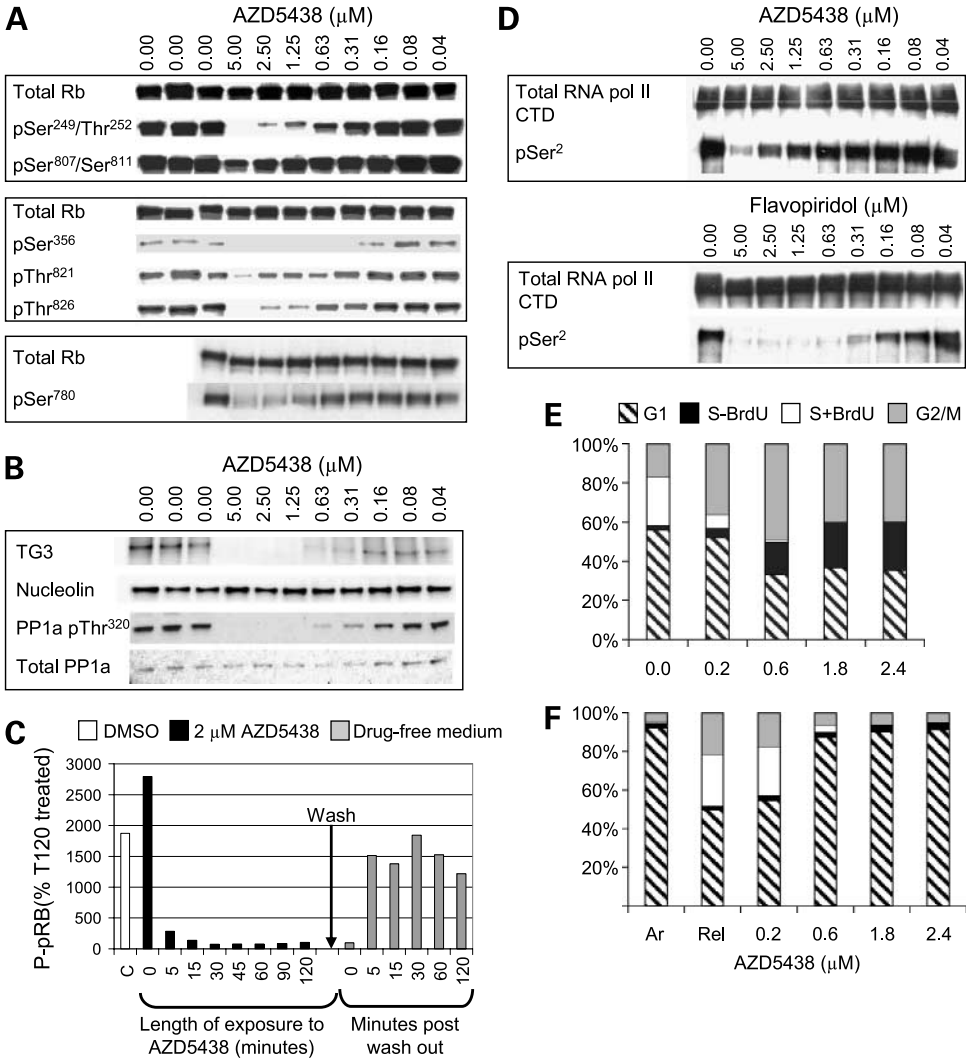

Figure 2. Mechanism of action of AZD5438 *in vitro*. **A,** asynchronously growing SW620 cells were dosed with a range of concentrations of AZD5438 or DMSO vehicle and the effect on phosphorylation status of the cdk2 substrate pRb measured by Western blotting using phosphospecific antibodies as indicated. **B,** SW620 cells were arrested in mitosis with nocodazole treatment for 16 h before treatment with AZD5438 for 2 h. The effect on phosphorylation of cdk1 substrates phosphonucleolin (*TG3* and *Nucleolin panels*) and PP1a (*bottom*) was measured. The data in **A** and **B** are representative of at least two independent experiments. **C,** the kinetics (*black columns*) and recovery (*gray columns*) of pRb phosphorylation ($pSer^{249}/pThr^{252}$) was further investigated in SW620 cells by exposing cells to 2 μmol/L AZD5438 for up to 2 h. Note that the pRb phosphorylation returned to near control levels within 5 min after removal of compound. Data are normalized to total pRb levels and expressed relative to the 2-h time point just before washout (%T120 treated). *White column C,* DMSO control. **D,** the ability of AZD5438 and flavopiridol to inhibit the activity of cdk9 was determined by measuring the phosphorylation of RNA polymerase II at the Ser^2 site in SW620 cells, treated as in **A**. **E,** fluorescence-activated cell sorting analysis of asynchronous MCF-7 cells treated with AZD5438 for 24 h showed an increase in the percentage of cells in G_2-M (*gray columns*) and a reduction in the proportion of S-phase cells undergoing active DNA synthesis as measured by BrdUrd incorporation (*black columns*). Gating was done as previously described (14). **F,** induction of a G_1 block (*columns with diagonal shading*) was revealed when MCF-7 cells were arrested in G_1 by serum withdrawal (*Arr*) and then released in the presence of drug for 24 h (*Rel*). All data are representative of at least two independent experiments.

concentration data was done using WinNonLin Professional (version 3.1; Pharsight Corp.).

Results

AZD5438 Is a Potent Inhibitor of cdks 1, 2, and 9

AZD5438 is a 4-(1-isopropyl-2-methylimidazol-5-yl)-2-(4-methylsulphonylanilino) pyrimidine (24). Analytic evidence as well as an X-ray crystal structure of the compound bound to cdk2 confirmed the structure (Fig. 1). AZD5438 potently inhibited the kinase activity of cyclin E-cdk2, cyclin A-cdk2, cyclin B1-cdk1, p25-cdk5, cyclin D3-cdk6, and cyclin T-cdk9 (IC_{50}, 6, 45, 16, 21, and 20 nmol/L, respectively) and was 75-fold less active against cyclin D-cdk4 (Table 1). AZD5438 was more potent against cdk2 and cdk1 than other drugs in the class, flavopiridol and R-roscovitine (Table 1). In common with many other cdk inhibitors, AZD5438 also inhibited the kinase activity of p25-cdk5 and glycogen synthase kinase 3β *in vitro* (IC_{50}, 14 and 17 nmol/L, respectively;

Table 2. Average IC_{50} values in μmol/L for AZD5438-mediated growth inhibition in a broad range of human tumor cell lines *in vitro*

Cell line	Description	Average IC_{50} (μmol/L)	SD	*n*
MCF-7	Breast	0.22	0.10	12
MCF-7AdR	Breast	0.31	ND	3
MDA-MB-231	Breast	0.46	0.06	5
HCT-116	Colon	0.32	0.08	7
HCT-15	Colon	1.13	0.22	3
HT29	Colon	1.05	0.72	8
LoVo	Colon	0.63	0.26	10
SW620	Colon	0.58	0.29	8
Colo-205	Colon	0.70	0.18	5
A549	Lung	0.57	0.08	3
NCI-H322	Lung	0.40	0.12	5
NCI-H460	Lung	0.87	0.19	6
PC-3	Prostate	0.20	0.07	4
DU145	Prostate	0.42	0.02	2
A2780	Ovarian	1.26	0.17	3
HeLa	Cervix	1.10	0.30	2
IM-9	Multiple myeloma	1.00	ND	1
MOLP-8	Multiple myeloma	1.10	ND	1
AMO-1	Plasmacytoma	1.00	ND	1
ARH-77	Plasma cell leukemia	1.70	ND	1
KARPAS-620	Plasma cell leukemia	0.74	ND	1
JJN-3	Plasma cell leukemia	0.94	ND	1
L-363	Plasma cell leukemia	0.50	ND	1

ref. 29). AZD5438 has not shown significant activity against 30 of 44 kinases tested in a commercially available panel (based on ≤75% inhibition at 10 μmol/L; see Supplementary Table S1).[4]

AZD5438 inhibited phosphorylation of the cdk1, cdk2, and cdk4 substrate retinoblastoma (pRb; Fig. 2A) and the cdk1 substrates nucleolin and PP1a in SW620 cells (Fig. 2B; refs. 30, 31). Studies were conducted in both asynchronous and nocodazole-blocked cells harvested following treatment with AZD5438 for 2 hours. As expected, there was a dose-dependent decline in phosphorylation on treatment with AZD5438, with an IC_{50} for inhibition of pRb phosphorylation at $Ser^{249}Thr^{252}$ approximately equal to the cellular IC_{50} for proliferation (compare Fig. 2A with IC_{50} data for SW620 in Table 2). Another NH_2-terminal phosphorylation site, Ser^{356}, was also particularly sensitive to AZD5438. The inability of AZD5438 to potently inhibit phosphorylation of the cdk4 phosphorylation sites Ser^{807}/Ser^{811} and Ser^{780} indicated that AZD5438 was not a potent inhibitor of cdk4 in cells. Kinetic studies of pRb phosphorylation at $Ser^{249}Thr^{252}$ revealed that >80% of pRb phosphorylation was inhibited within 5 minutes of treatment with 2 μmol/L AZD5438 and the effect was rapidly reversed on removal of the drug (Fig. 2C). The ability of AZD5438 to inhibit the activity of cdk9 was determined by measuring the phosphorylation of RNA polymerase II at the Ser^2 site in SW620 cells (Fig. 2D). A dose-dependent inhibition of Ser^2 phosphorylation was observed, with relatively higher concentrations of drug required to achieve 50% inhibition, compared with other cdk substrates.

AZD5438 Induces Cell Cycle Arrest Consistent with Its Activity against cdks

By phosphorylating and regulating the activity of pRb, cdk2 plays a role in controlling the restriction point governing the G_1-S transition. During S phase, cdk2 regulates the appropriate timing of E2F-1 activity and is involved in the initiation of DNA synthesis at origins of replication (32–34). Cyclin A-cdk2 activity persists into G_2 phase where it mediates entry into mitosis (35). Cyclin B1-cdk1 phosphorylates numerous proteins involved in the regulation of mitosis (36). This suggests that small-molecule dual cdk1/cdk2 inhibitors will arrest cells in G_1, S, and G_2-M and lead to inhibition of DNA synthesis in S phase. In common with other cdk1/cdk2 inhibitors (14), AZD5438 induced blocks in G_2-M and S phase in MCF-7 cells with concomitant inhibition of DNA synthesis as measured by BrdUrd incorporation (Fig. 2E). The inhibition of DNA synthesis occurred throughout S phase as suggested by the presence of cells with intermediate DNA content that had completely stopped replicating DNA (S-BrdUrd population in Fig. 3).

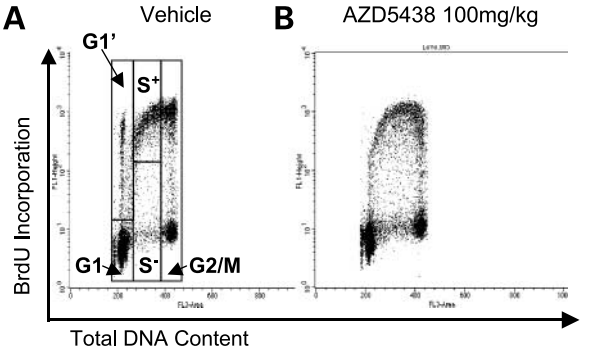

C

Percentage of cells in cell cycle phases					
Treatment	**%G1'**	**%G1**	**%S-**	**%S+**	**%G2/M**
Vehicle 6h	3.8	60.8	9.4	6.4	23.3
AZD5438 6h	0.0	60.0	8.4	8.1	23.5

Figure 3. AZD5438 treatment *in vivo* leads to antiproliferative effects. Female nude mice were s.c. implanted with SW620 tumors. When tumors became palpable, animals were orally dosed with either vehicle or AZD5438, and after 2 h of treatment, mice were injected i.p. with BrdUrd. Subgroups of mice (n = 3/group/time point) were removed during experiments and cell suspensions were prepared from dissected tumors and analyzed for BrdUrd incorporation/cell cycle kinetics using flow cytometry as described in Materials and Methods. **A,** typical dot plot indicating that vehicle-treated tumor cells are able to complete cell cycle and progress to the G1′ stage. **B,** effects on the G1′ population *in vivo* following AZD5438 (100 mg/kg) treatment. **C,** summary of comparative analysis of **A** versus **B** results.

[4] Supplementary material for this article is available at Molecular Cancer Therapeutics Online (http://mct.aacrjournals.org/).

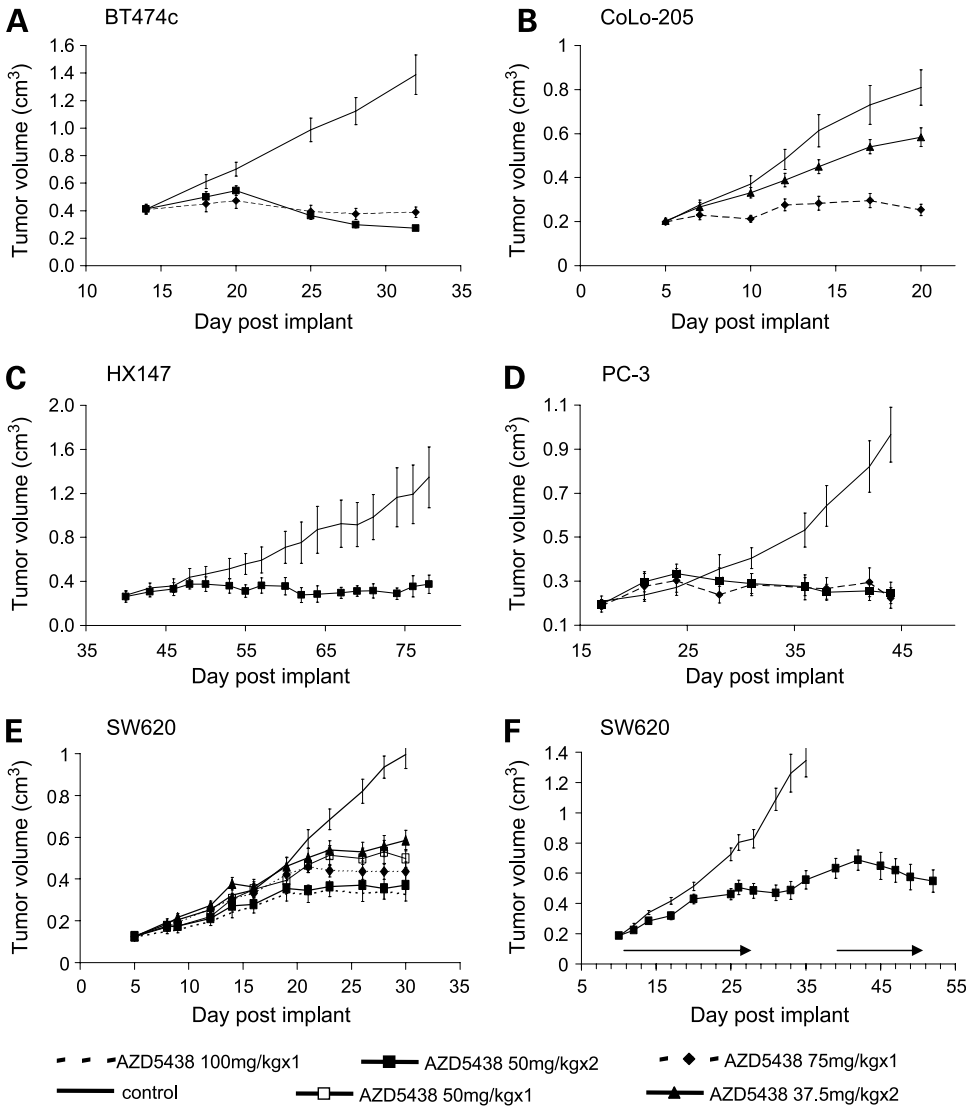

Figure 4. AZD5438 inhibits growth in a panel of human tumor xenografts. Female nude mice bearing established BT474c (**A**), Colo-205 (**B**), HX147 (**C**), PC-3 (**D**), and SW620 (**E** and **F**) human tumor xenografts were dosed by oral gavage daily (either once or twice daily) with either vehicle or AZD5438 at a range of doses indicated. *Points,* mean tumor volume (cm^3) of 8 to 10 mice; *bars,* SE. **F,** *arrows,* period of dosing.

Similar results were obtained in asynchronous LoVo and SW620 cells treated with AZD5438 (data not shown). Induction of a G_1 block was revealed when MCF-7 cells arrested in G_0-G_1 by serum withdrawal were released in the presence of drug (Fig. 2F).

AZD5438 Is Antiproliferative in a Range of Tumor Cell Lines

AZD5438 is a potent inhibitor of cell cycle cdk1 and cdk2, resulting in loss of phosphorylation of cdk-dependent substrates and multiple blocks in cell cycle in treated cells. Agents of this type are predicted to have broad activity across multiple tumor types. AZD5438 has been widely tested in proliferation assays in several cell panels representing lung, colorectal, breast, prostate, and hematologic tumors. Representative data are shown in Table 2. The IC_{50} values for inhibition of cellular proliferation across this panel ranged from 0.2 μmol/L (MCF-7) to 1.7 μmol/L (ARH-77). The range of differential sensitivity of cell lines across the panels to AZD5438 was moderate and could equally reflect differences in molecular pathology as proliferation rates of the cell lines studied; however, none of the cell lines was considered to be resistant to AZD5438.

AZD5438 Treatment of Human Tumor Xenografts Inhibits Cell Cycle Progression

AZD5438 displayed physical and pharmacokinetic properties suitable for *in vivo* preclinical studies. To measure the effect of AZD5438 treatment on the progression of tumor cells through the cell cycle *in vivo*, immunodeficient mice implanted s.c. with SW620 tumors (human colorectal) were treated with either vehicle alone or AZD5438 and pulsed with BrdUrd (200 mg/kg, i.p.) to label cycling cells at t = 0 hour. After culling of the animals at t = 6 hours, the lysates generated from excised tumors were analyzed using flow cytometry as for the *in vitro* studies. Typical control data generated in this model are shown in Fig. 3A. During the

time course of the study, a significant population of cells incorporated the BrdUrd label during S phase and a proportion of these cells transited through mitosis to return to G_1. These cells can be seen in the flow cytometric analysis as a distinctive BrdUrd-positive "spike" above the unlabeled G_1 population (labeled G1′ in Fig. 3A). AZD5438 showed a clear halt in progression through the cell cycle in this model, as determined by a reduction in the G1′ population (Fig. 3B and C). Similar cell cycle effects have been observed in other human tumor lines *in vivo*, including PC-3 (prostate); HCT-15, HCT-116, and LoVo (all colorectal); and A2780 (ovarian; data not shown). Kinetic studies in LoVo xenografts indicated a prolonged inhibition of cells progressing through the cell cycle to G1′ after a single dose of AZD5438 (100 mg/kg, orally), where the G1′ population remained at ~50% of vehicle controls at 15 hours.

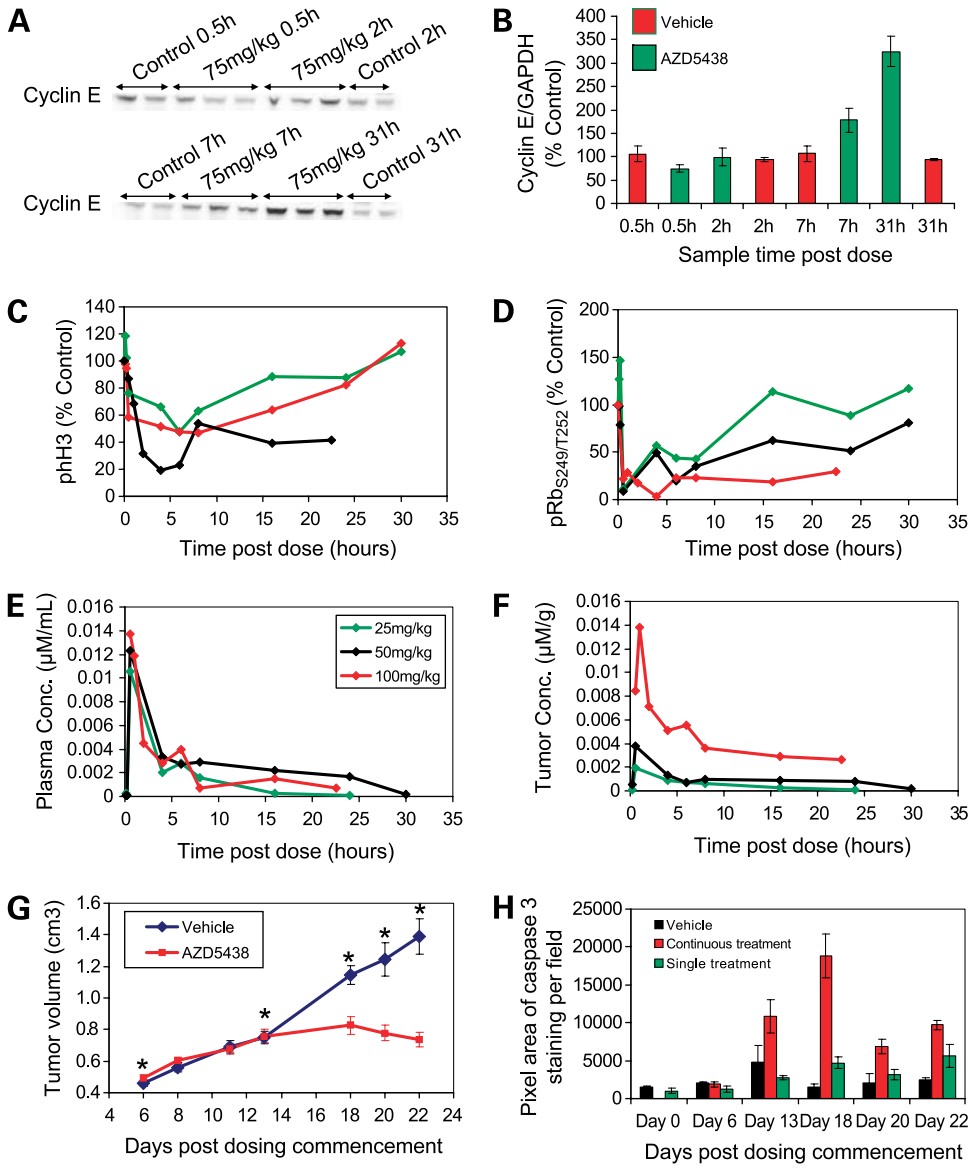

Figure 5. Temporal pharmacodynamic analysis of AZD5438-sensitive tumor xenografts. AZD5438 treatment leads to phenotypic and biomarker changes in tumor xenografts. SW620 tumor xenografts were established in female nude mice and treated orally with vehicle alone or AZD5438, as described in Materials and Methods. Cyclin E protein levels following a single administration of AZD5438 (75 mg/kg). Data indicate Western blot (each band representing a separate individual xenograft; **A**) and quantification by densitometry (**B**). Pharmacokinetic/pharmacodynamic responses following a single administration of AZD5438 (25, 50, and 100 mg/kg). Data indicate phH3 (by flow cytometry; **C**) and phospho-pRb $pSer^{249}/pThr^{252}$ (by Western blot; **D**). Concentrations of AZD5438 are shown for plasma (μmol/L/mL; **E**) and tumor (μmol/L/g; **F**). **G** and **H,** SW620 tumors were given single or continuous treatment of AZD5438 (once daily, 75 mg/kg). Animals receiving continuous treatment were sampled on day of dosing commencement (day 0) and then subsequently on days 6, 13, 18, 20, and 22 (*). Additional subgroups received only a single dose of AZD5438 and were also sampled on these days. TGI response of animals completing 22 d of treatment (n = 10 per group; **G**) and quantitative analysis by scanning microscopy of cleaved caspase-3–immunostained tumors (**H**), as described in Materials and Methods. Unless otherwise stated, the above pharmacodynamic data represent n = 3 animals per group per time point. *Bars,* SE.

Table 3. Relationship between pharmacodynamic biomarkers and TGI in the SW620 xenograft model

Dose of AZD5438 (mg/kg)	Maximum % TGI*	% Inhibition of pRb pSer^{249}/pThr^{252} phosphorylation at 16 h after dose†,‡	AZD5438 tumor concentration in μg/g (μmol/L/g)†	AZD5438 plasma concentration in μg/mL (μmol/L/mL)†
100	75	82	1.35 (0.0029)	0.7 (0.0015)
50	58	49	0.4 (0.0009)	1.04 (0.0022)
25	32	12	0.14 (0.0003)	0.14 (0.0003)

*SW620 xenografts were established and then treated with vehicle alone or AZD5438 (once a day, orally) for 3 wk; maximum %TGI values, representing $n = 10$ per treatment group, were calculated as described in Materials and Methods.
†Data generated 16 h after a single dose oral of AZD5438 ($n = 3$ treatment group).
‡Phospho-Rb$^{S249/T252}$ percentage inhibition calculated versus vehicle-dosed control.

AZD5438 Inhibits the Growth of Human Tumor Xenografts

AZD5438 was chronically dosed (once or twice daily orally at a range of doses) and tested for efficacy in immunodeficient rodents s.c. implanted with human tumor xenografts derived from a wide range of different cancer types (e.g., breast, colon, lung, prostate, and ovarian; Supplementary Table S2).[4] Statistically significant TGI was observed against all models screened (maximum % TGI range, 38–153%; $P < 0.05$; Fig. 4A–E; Supplementary Table S2).[4] Greater than 40% inhibition was seen with all the tumor xenografts dosed at 75 mg/kg/d, with the human breast xenograft BT474c showing inhibition of tumor growth by up to 124% (Fig. 4A). The SW620 model was used to investigate several aspects of dosing regimens with AZD5438. Clear dose responses to AZD5438 were observed (Fig. 4E). Therapy withdrawal studies indicated that antitumor activity could be reinstated following drug-free periods of AZD5438 (Fig. 4F).

Temporal Pharmacodynamic Analysis of AZD5438-Sensitive Tumor Xenografts

Analysis of AZD5438-treated xenografts (SW620) indicated responsiveness with several cell cycle proteins. For example, phH3, phosphonucleolin, PP1a, and several phospho-pRb epitopes showed decreased levels in AZD5438-treated tumors when compared with vehicle-treated controls (data not shown). Western blot analysis of tumor samples for cyclin E showed elevated levels following AZD5438 treatment compared with vehicle controls (Fig. 5A and B).

A pharmacokinetic/pharmacodynamic study was undertaken in the SW620 tumor model to establish a relationship between exposure to AZD5438 and expression of cell cycle markers. Tumor-bearing mice were given a single bolus dose of AZD5438 (25, 50, or 100 mg/kg, orally) and subgroups of animals were culled and analyzed for pharmacodynamic effects. Analysis of phospho-pRb pSer^{249}/pThr^{252} by Western blot showed that the biomarker rapidly declined in response to AZD5438 exposure in all treatment groups. The largest effect was observed with the highest dose of AZD5438, with tumors treated with 100 mg/kg remaining having suppressed phospho-pRb pSer^{249}/pThr^{252} up to the final sample point (Fig. 5C). Similarly, levels of phH3 (by flow cytometry), a marker of mitosis, declined and had not recovered by 50% at the 22.5-hour time point in the 100 mg/kg AZD5438–treated group (Fig. 5D). Pharmacokinetic analysis of plasma and tumor total AZD5438 concentrations, from the same study, indicated a clear dose response (Fig. 5E and F, respectively). We further explored the relationship between pharmacodynamic factors and therapeutic outcome by comparing phospho-pRb pSer^{249}/pThr^{252} with percentage growth inhibition after different chronic dosing regimens of AZD5438 in the SW620 xenograft model. The results are summarized in Table 3.

In a separate SW620 study, the longer-term effects of AZD5438 treatment were analyzed (Fig. 5G). Staining and quantification of tumor samples on days 0, 6, 13, 18, 20, and 22 for the apoptotic marker cleaved caspase-3 showed elevated levels (compared against vehicle control) only after ~2 weeks of chronic AZD5438 treatment (days 13 and 18; Fig. 5H). To determine whether the effects were the result of chronic AZD5438 treatment, on each of the sample days a subgroup of animals, which had only received just a single dose of AZD5438 on that particular day, was also taken. Although the AZD5438 single-dose subgroup of animals showed effects on cell cycle (as determined by BrdUrd incorporation; data not shown), there was little evidence of apoptosis when compared with the corresponding AZD5438 chronic dose group (Fig. 5H).

Discussion

The activity of AZD5438 against cdk1, cdk2, and cdk9 offers an attractive therapeutic strategy in the context of recent data, suggesting that, *in vitro*, certain tumor cell lines can survive specific inhibition of cdk2 (9, 37) and, *in vivo*, there seems to be redundancy among cell cycle cdks (reviewed in ref. 7). *In vitro*, AZD5438 was a potent inhibitor of cyclin B1-cdk1, cyclin E-cdk2, and cyclin A-cdk2, where IC_{50}s against recombinant enzymes were in the low nanomolar range at K_m ATP (see Table 1). Cellular potency was shown in SW620 cells, where AZD5438 inhibited proliferation and inhibited phosphorylation of cdk-specific substrates. The IC_{50} for inhibition of proliferation of the SW620 cell line was 0.6 μmol/L, which was sufficient to inhibit phosphorylation of key substrates in these cells, including pRb pSer^{249}/pThr^{252}, pRb pThr^{356}, phosphonucleolin, and PP1a pThr^{320} by at least 50% (see Fig. 2A and B). This suggests that the primary mechanism of action of AZD5438 is cdk inhibition leading to growth inhibition, consistent with the observation of an antiproliferative effect in multiple cell lines.

Regulation of G_1-S phase progression by pRb is primarily a function of its ability to interact with E2F transcription factors and to repress E2F-responsive promoters leading to growth suppression. Several phosphorylation sites on pRb regulate its interaction with other proteins including E2F (Ser^{780} and Ser^{795}), proteins containing LXCXE motifs (Thr^{821} and Thr^{826}; refs. 38, 39), and cAbl (Ser^{807}/Ser^{811}; refs. 39, 40). These sites all lie in the COOH-terminal region (amino acids 792–928) and the conserved central pocket (amino acids 379–792) that are essential for pRb activity. Our analysis suggests that Ser^{780} is relatively refractory to AZD5438, which may reflect the fact that this site (together with Ser^{795}) is phosphorylated by several kinases, including cyclin D–dependent kinases (41), extracellular signal-regulated kinase 1/2 (42), and transglutaminase 2 kinase (43). Cyclin D1-cdk4 mediates phosphorylation of pRb on Ser^{807}/Ser^{811} (39, 40) and Thr^{826}, whereas Thr^{821} is phosphorylated by both cdk2 and cdk6 (38, 39). Two cdk phosphorylation sites that were particularly sensitive to AZD5438 (Ser^{249} and Thr^{252}) lie in the arginine-rich linker connecting cyclin fold helices 3 and 4 of the RbN B lobe (44). Phosphorylation at these sites by either cyclin B-cdk1 or cyclin A-cdk2 was shown to block binding of the ligand EID-1 (44). Further evidence that the NH_2-terminal domain of pRb is functionally important comes from the recent observation that pRb inactivation can be mediated by cyclin E-cdk phosphorylation of a single site (Thr^{373}; ref. 45). This site was also sensitive to AZD5438, raising the possibility that AZD5438 could interfere with functionality of the NH_2-terminal domain of pRb by inhibiting phosphorylation of key sites and hence altering ligand binding and RbN-pocket domain interactions.

Consistent with these data, AZD5438 induced blocks in G_2-M and S phase in asynchronously growing MCF-7 cells and potently inhibited DNA replication (measured by BrdUrd incorporation) at 0.2 μmol/L, the IC_{50} for proliferation in these cells. Further studies revealed a G_1 block when MCF-7 cells were synchronized by release from serum starvation in the presence of AZD5438; however, the concentration of AZD5438 required to induce a G_1 arrest was higher than that which produced blocks in S and G_2 (compare the 0.2 μmol/L dose in Fig. 2E and F), likely reflecting the fact that although AZD5438 was found to be a potent inhibitor of cdk6, it was also significantly less active against cdk4 and therefore less able to induce a G_1 block. Overall, the cell cycle profile induced by AZD5438 is consistent with its ability to potently inhibit cdk1 and cdk2 as described in Table 1. Because AZD5438 was also active against recombinant cyclin T-cdk9, we examined the ability of AZD5438 to inhibit phosphorylation of the cdk9/pTEFβ substrate, Ser^2 of the CTD of RNA polymerase II. When compared with flavopiridol, AZD5438 was less effective at inhibiting phosphorylation at Ser^2, and higher concentrations of drug (~5 μmol/L) were required to inhibit 50% of control phosphorylation. This was somewhat surprising, given how similar the IC_{50}s for flavopiridol and AZD5438 are for recombinant cdk9 (20 and 11 nmol/L, respectively), and may reflect differences in the inherent sensitivity of these assays. AZD5438 inhibited the activity of cdk5, a known regulator of migration in neuronal development. Although there is limited evidence for the involvement of cdk5 in the development of cancer, it has been shown that cdk5 plays a role in regulating motility and metastatic potential of prostate cancer cells (46). Further, the ability of roscovitine to inhibit proliferation and induce apoptosis in the invasive breast cancer cell line MDA-MB-231 may at least in part be explained by its ability to inhibit cdk5 (47). These data suggest that any effect of AZD5438 on cdk5 is worthy of further investigation. Recent studies that define the optimal combination of cdk targets to mediate killing of tumor cell lines found that combined depletion of cdk1 and cdk2 either by genetic or chemical means induced a more potent antiproliferative effect than depletion of either cdk alone, which was further enhanced by combined cdk9 inhibition (9, 48). Taken together, these data suggest that inhibitors targeting multiple cdks may be more effective at inducing apoptosis in tumor cells than selective agents targeted at single cdks.

AZD5438 significantly inhibited the growth of a range of tumors *in vivo* with an efficacious dose of 75 mg/kg/d. The effects of AZD5438 were dose and schedule dependent, with maximum antitumor activity requiring a continuous daily dosing schedule. Moreover, in an acute pharmacodynamic model, treatment with AZD5438 inhibited the progression of cells from the G_2-M into S phase, achieving sufficient tumor and plasma drug concentrations to inhibit cdk activity in tumor xenografts as evidenced by inhibition of pRb phosphorylation and an increase in the total level of cyclin E. The loss of histone H3 phosphorylation at Ser^{10} provided further evidence of cell cycle inhibition in this *in vivo* model.

The relationship between pharmacokinetic/pharmacodynamic and antitumor activity was further examined by comparing different chronic dosing regimens of AZD5438 and efficacy readouts in the SW620 xenograft model. The summary results indicate that efficacious doses of AZD5438 (>40% TGI) maintained suppression of biomarkers (phospho-pRb $pSer^{249}/pThr^{252}$ and phH3) for at least 16 hours following a single dose with tumor concentrations of AZD5438 at this time point being equivalent to 0.4 μg/g (0.0009 μmol/L/g). The effect of AZD5438 on pRb phosphorylation *in vivo* tracked with both plasma and tumor concentrations of the drug and was dose dependently reversible with somewhat slower kinetics than that observed *in vitro*. In scheduling studies, we observed that AZD5438 did not inhibit tumor growth when dosed every other day (data not shown), indicating that continuous inhibition of the target cdks was required. Interestingly, longer-term biomarker studies in SW620 xenografts indicated that, as well as cell cycle arrest, AZD5438 treatment could lead to increased apoptosis.

AZD5438 was being developed for the treatment of a range of solid tumors. Phase I clinical studies revealed a well-tolerated agent at up to 80 mg administered as single oral doses. The dose-limiting adverse events were nausea and vomiting (49). A further, previously reported phase I clinical study, in which the pharmacodynamic activity of AZD5438

was evaluated (23), showed that the ratio of phospho-pRb/total pRb was significantly reduced 1.5 hours after 40 and 80 mg AZD5438 compared with placebo. No significant differences were noted at 6 hours after dosing, consistent with the plasma $t_{1/2}$ of 1 to 3 hours and the rapid reversibility of pRb phosphorylation previously seen on cessation of dosing in preclinical studies. These data support a close pharmacokinetic-pharmacodynamic relationship between AZD5438 and target inhibition, and to further understand this relationship, we built a predictive pharmacokinetic/pharmacodynamic model that describes the time course of changes in pRb phosphorylation following administration of AZD5438.[5] This model was adapted and combined with early human pharmacokinetic data (see ref. 49) to predict pRb response in buccal samples from healthy volunteers in the pharmacodynamic study described above (23). The closeness of the prediction from the model to the observed data suggested similarities in biomarker response to pRb between human xenograft cells implanted in nude mice and human buccal cells in healthy volunteers. Taken together, our studies with AZD5438 support the view that cdk inhibition is an attractive therapeutic approach for solid tumors. Optimal dosing regimens should aim to achieve a well-tolerated pharmacologically relevant exposure level and maintain this exposure for 16 hours (or about one cell cycle).

AZD5438 has provided preclinical evidence in this current study, and clinical evidence elsewhere (23), that broad-spectrum rather than targeted cdk inhibition may be more likely to provide therapeutic benefit. The clinical development program for AZD5438 was discontinued due to a lack of tolerability and high variability in phase II studies in patients, thereby preventing further proof-of-concept studies for this agent. In conclusion, AZD5438 is an orally active inhibitor of cdk1, cdk2, and cdk9 offering good selectivity against a range of other kinases and biological targets.

[5] M. Walker, in preparation.

Disclosure of Potential Conflicts of Interest

All authors are employees of and own stock in AstraZeneca.

Acknowledgments

We thank the AZD5438 chemistry team for kindly providing compounds; Francoise Powell, Lisa Drew, Benjamin Caleb, and Mark Roth for *in vitro* data; Sharon Barnett, Nicola Haupt, David Smith, Julie Humphreys, Keith Welsh, Darren Harrison, and Nigel Leake for technical assistance; John Foster and Alison Bigley for histologic support; Joanne Wilson for bioanalysis; Dereck Amakye, Donna Johnstone, and Andrew Hughes for translational science input; Steve Wedge for technical discussions, and Sonya Zabludoff and Blaze Stancampiano for critical reading of the manuscript.

References

1. Ortega S, Malumbres M, Barbacid M. Cyclin D-dependent kinases, INK4 inhibitors and cancer. Biochim Biophys Acta 2002;1:73–87.

2. Barton MC, Akli S, Keyomarsi K. Deregulation of cyclin E meets dysfunction in p53: closing the escape hatch on breast cancer. J Cell Physiol 2006;209:686–94.

3. Lopez-Beltran A, MacLennan GT, Montironi R. Cyclin E as molecular marker in the management of breast cancer: a review. Anal Quant Cytol Histol 2006;28:111–14.

4. Shapiro GI. Cyclin-dependent kinase pathways as targets for cancer treatment. J Clin Oncol 2006;24:1770–783.

5. Malumbres M, Barbacid M. Mammalian cyclin-dependent kinases. Trends Biochem Sci 2005;30:630–41.

6. Santamaria D, Ortega S. Cyclins and CDKS in development and cancer: lessons from genetically modified mice. Front Biosci 2006;11:1164–88.

7. Aleem E, Kaldis P. Mouse models of cell cycle regulators: new paradigms. Results Probl Cell Differ 2006;42:271–328.

8. Aleem E, Kiyokawa H, Kaldis P. Cdc2-cyclin E complexes regulate the G_1/S phase transition. Nat Cell Biol 2005;7:831–36.

9. Cai D, Latham VM, Jr., Zhang X, Shapiro GI. Combined depletion of cell cycle and transcriptional cyclin-dependent kinase activities induces apoptosis in cancer cells. Cancer Res 2006;66:9270–80.

10. Fry DW, Harvey PJ, Keller PR, et al. Specific inhibition of cyclin-dependent kinase 4/6 by PD 0332991 and associated antitumor activity in human tumor xenografts. Mol Cancer Ther 2004;3:1427–38.

11. Chen YN, Sharma SK, Ramsey TM, et al. Selective killing of transformed cells by cyclin/cyclin-dependent kinase 2 antagonists. Proc Natl Acad Sci U S A 1999;96:4325–29.

12. Byth KF, Cooper N, Culshaw JD, et al. Imidazo[1,2-*b*]pyridazines: a potent and selective class of cyclin-dependent kinase inhibitors. Bioorg Med Chem Lett 2004;14:2249–52.

13. Byth KF, Culshaw JD, Green S, Oakes SE, Thomas AP. Imidazo[1,2-*a*] pyridines. Part 2. SAR and optimisation of a potent and selective class of cyclin-dependent kinase inhibitors. Bioorg Med Chem Lett 2004;14: 2245–48.

14. Byth KF, Geh C, Forder CL, Oakes SE, Thomas AP. The cellular phenotype of AZ703, a novel selective imidazo[1,2-*a*]pyridine cyclin-dependent kinase inhibitor. Mol Cancer Ther 2006;5:655–64.

15. Zaffaroni N, Pennati M, Daidone MG. Survivin as a target for new anticancer interventions. J Cell Mol Med 2005;9:360–72.

16. Goga A, Yang D, Tward AD, Morgan DO, Bishop JM. Inhibition of CDK1 as a potential therapy for tumors over-expressing MYC. Nat Med 2007;13:820–27.

17. Marshall RM, Grana X. Mechanisms controlling CDK9 activity. Front Biosci 2006;11:2598–613.

18. Peterlin BM, Price DH. Controlling the elongation phase of transcription with P-TEFb. Mol Cell 2006;23:297–305.

19. Fisher RP. Secrets of a double agent: CDK7 in cell-cycle control and transcription. J Cell Sci 2005;118:5171–180.

20. Cisek LJ, Corden JL. Phosphorylation of RNA polymerase by the murine homologue of the cell-cycle control protein cdc2. Nature 1989;339: 679–84.

21. Deng L, Ammosova T, Pumfery A, Kashanchi F, Nekhai S. HIV-1 Tat interaction with RNA polymerase II C-terminal domain (CTD) and a dynamic association with CDK2 induce CTD phosphorylation and transcription from HIV-1 promoter. J Biol Chem 2002;277:33922–929.

22. Byrd JC, Lin TS, Dalton JT, et al. Flavopiridol administered using a pharmacologically derived schedule is associated with marked clinical efficacy in refractory, genetically high-risk chronic lymphocytic leukemia. Blood 2007;109:399–404.

23. Camidge DR, Pemberton M, Growcott J, et al. A phase I pharmacodynamic study of the effects of the cyclin-dependent kinase-inhibitor AZD5438 on cell cycle markers within the buccal mucosa, plucked scalp hairs and peripheral blood mononucleocytes of healthy male volunteers. Cancer Chemother Pharmacol 2007;60:479–88.

24. Anderson M, Andrews DM, Barker AJ, et al. Imidazoles: SAR and development of a potent class of cyclin-dependent kinase inhibitors. Bioorg Med Chem Lett 2008;18:5487–92.

25. Dranovsky A, Vincent I, Gregori L, et al. Cdc2 phosphorylation of nucleolin demarcates mitotic stages and Alzheimer's disease pathology. Neurobiol Aging 2001;22:517–28.

26. Wedge SR, Ogilvie DJ, Dukes M, et al. ZD4190: an orally active inhibitor of vascular endothelial growth factor signaling with broad-spectrum antitumor efficacy. Cancer Res 2000;60:970–75.

27. Wilkinson RW, Odedra R, Heaton SP, et al. AZD1152, a selective inhibitor of Aurora B kinase, inhibits human tumor xenograft growth by inducing apoptosis. Clin Cancer Res 2007;13:3682–88.

28. McKillop D, Partridge EA, Kemp JV, et al. Tumor penetration of gefitinib (Iressa), an epidermal growth factor receptor tyrosine kinase inhibitor. Mol Cancer Ther 2005;4:641–9.

29. Leclerc S, Garnier M, Hoessel R, et al. Indirubins inhibit glycogen synthase kinase-3β and CDK5/p25, two protein kinases involved in abnormal τ phosphorylation in Alzheimer's disease. A property common to most cyclin-dependent kinase inhibitors? J Biol Chem 2001;276:251–60.

30. Belenguer P, Caizergues-Ferrer M, Labbe JC, Doree M, Amalric F. Mitosis-specific phosphorylation of nucleolin by p34cdc2 protein kinase. Mol Cell Biol 1990;10:3607–18.

31. Dohadwala M, da Cruz e Silva EF, Hall FL, et al. Phosphorylation and inactivation of protein phosphatase 1 by cyclin-dependent kinases. Proc Natl Acad Sci U S A 1994;91:6408–12.

32. Coverley D, Laman H, Laskey RA. Distinct roles for cyclins E and A during DNA replication complex assembly and activation. Nat Cell Biol 2002;4:523–28.

33. Harper JW, Adams PD. Cyclin-dependent kinases. Chem Rev 2001;101:2511–26.

34. Sherr CJ, Roberts JM. CDK inhibitors: positive and negative regulators of G_1-phase progression. Genes Dev 1999;13:1501–12.

35. Hu B, Mitra J, van den Heuvel S, Enders GH. S and G_2 phase roles for Cdk2 revealed by inducible expression of a dominant-negative mutant in human cells. Mol Cell Biol 2001;21:2755–66.

36. Castedo M, Perfettini JL, Roumier T, Kroemer G. Cyclin-dependent kinase-1: linking apoptosis to cell cycle and mitotic catastrophe. Cell Death Differ 2002;9:1287–93.

37. Tetsu O, McCormick F. Proliferation of cancer cells despite CDK2 inhibition. Cancer Cell 2003;3:233–45.

38. Takaki T, Fukasawa K, Suzuki-Takahashi I, et al. Preferences for phosphorylation sites in the retinoblastoma protein of D-type cyclin-dependent kinases, Cdk4 and Cdk6, *in vitro*. J Biochem 2005;137:381–86.

39. Zarkowska T, Mittnacht S. Differential phosphorylation of the retinoblastoma protein by G_1/S cyclin-dependent kinases. J Biol Chem 1997;272:12738–46.

40. Knudsen ES, Wang JYJ. Differential regulation of retinoblastoma protein function by specific Cdk phosphorylation sites. J Biol Chem 1996;271:8313–20.

41. Connell-Crowley L, Harper JW, Goodrich DW. Cyclin D1/Cdk4 regulates retinoblastoma protein-mediated cell cycle arrest by site-specific phosphorylation. Mol Biol Cell 1997;8:287–301.

42. Guo J, Sheng G, Warner BW. Epidermal growth factor-induced rapid retinoblastoma phosphorylation at Ser^{780} and Ser^{795} is mediated by ERK1/2 in small intestine epithelial cells. J Biol Chem 2005;280:35992–8.

43. Mishra S, Melino G, Murphy LJ. Transglutaminase 2 kinase activity facilitates protein kinase A-induced phosphorylation of retinoblastoma protein. J Biol Chem 2007;282:18108–15.

44. Hassler M, Singh S, Yue WW, et al. Crystal structure of the retinoblastoma protein N domain provides insight into tumor suppression, ligand interaction, and holoprotein architecture. Mol Cell 2007;28:371–85.

45. Lents NH, Gorges LL, Baldassare JJ. Reverse mutational analysis reveals threonine-373 as a potentially sufficient phosphorylation site for inactivation of the retinoblastoma tumor suppressor protein (pRB). Cell Cycle 2006;5:1699–707.

46. Strock CJ, Park J-I, Nakakura EK, et al. Cyclin-dependent kinase 5 activity controls cell motility and metastatic potential of prostate cancer cells. Cancer Res 2006;66:7509–15.

47. Goodyear S, Sharma MC. Roscovitine regulates invasive breast cancer cell (MDA-MB231) proliferation and survival through cell cycle regulatory protein cdk5. Exp Mol Pathol 2007;82:25–32.

48. Cai D, Byth KF, Shapiro GI. AZ703, an imidazo[1,2-*a*]pyridine inhibitor of cyclin-dependent kinases 1 and 2, induces E2F-1-dependent apoptosis enhanced by depletion of cyclin-dependent kinase 9. Cancer Res 2006;66:435–44.

49. Camidge DR, Smethurst D, Growcott J, et al. A first-in-man phase I tolerability and pharmacokinetic study of the cyclin-dependent kinase-inhibitor AZD5438 in healthy male volunteers. Cancer Chemother Pharmacol 2007;60:391–98.